COGNITIVE NEUROSCIENCE
https://doi.org/10.1080/17588928.2026.2665610

Routledge
Taylor & Francis Group

Catching the drift: EEG microstate dynamics resemble time-on-task changes in mind wandering and sustained attention

Jason S. Tsukahara[a], Anthony P. Zanesco[b], Brooke Schwartzman[c], Ekaterina Denkova[a] and Amishi P. Jha[a]

[a]Department of Psychology, University of Miami, Coral Gables, FL, USA; [b]Department of Psychology, University of Kentucky, Lexington, KY, USA; [c]Department of Psychology, Florida State University, Tallahassee, FL, USA

ABSTRACT

Sustained focus is essential for effective goal-directed behavior. Yet, as sustained attention tasks drag on, the occurrence of mind wandering increases. Recent studies suggest that such increases in mind wandering correspond with increases in response time variability and declines in accuracy with greater time-on-task. Relatively little is known about how large-scale brain dynamics unfold over similar timescales. EEG microstates offer a way to characterize these dynamics by capturing brief, quasi-stable topographical patterns that index distinct large-scale neural configurations. Prior work has shown that microstate C corresponds with episodes of mind wandering, whereas microstate E corresponds with task-focused periods. The present study asked whether the prominence of these microstates may systematically shift with greater time-on-task. Thirty-four adults completed a 45-min Sustained Attention to Response Task, while EEG was recorded and canonical microstates were extracted. In line with established behavioral findings, self-reported mind wandering and performance indices suggested poorer task-focus with longer time-on-task. Critically, microstate metrics revealed a gradual increase in the prominence of microstate C (greater time coverage and occurrence) over the course of the task and a corresponding decrease in the prominence of microstate E (shorter duration). These results indicate that EEG microstate dynamics are sensitive to time-on-task related changes in sustained attention and track a shift from externally oriented task focus toward internally oriented, mind wandering states.

ARTICLE HISTORY
Received 29 December 2025
Revised 20 March 2026

KEYWORDS
EEG microstates; mind wandering; sustained attention; vigilance decrement

Attentional control is essential for goal-directed behavior, allowing individuals to resist distraction and remain engaged with ongoing tasks. Yet, maintaining attentional control over time is influenced by factors such as arousal, motivation, the availability of control resources, and the tendency to mind wander (Esterman & Rothlein, 2019). In particular, mind wandering, the disruptive occurrence of off-task thought during an ongoing task or activity, is a common influence on continued task performance. As task engagement is prolonged, individuals increasingly report that their attention drifts away from the task at hand toward task-unrelated thoughts (Thomson et al., 2015; Zanesco et al., 2025). Moreover, increases in mind wandering with greater time-on-task have been shown to co-vary with declines in accuracy and increases in response time variability (Zanesco et al., 2024). Together, these co-occurring changes in mind wandering and performance suggest that lapses in sustained attention frequently originate from ongoing shifts between externally and internally directed cognitive states.

The brain systems associated with these shifts have been proposed to correspond to dynamic interactions between large-scale brain networks implicated in goal-directed external task focus and internally focused cognition. Studies have shown that directing attention outward, toward external tasks, engages task-positive fMRI-derived networks while suppressing default mode network (DMN) activity (Raichle, 2015). These opposing activity patterns suggest that the DMN supports internally directed thought by insulating associative, stimulus-independent processes like mind wandering from external sensory influences (Margulies et al., 2016). Although fMRI studies have revealed large-scale network dynamics associated with mind wandering and lapses of attention, including changes within and between default mode and attention networks (Christoff et al., 2009; Fox et al., 2015; Weissman et al., 2006; Zhang et al., 2022), the slow temporal resolution of the hemodynamic response constrains the study of rapid neural transitions through which attentional states fluctuate.

CONTACT Amishi P. Jha a.jha@miami.edu Department of Psychology, University of Miami, 5665 Ponce de Leon, Coral Gables, FL 33146, USA
Supplemental data for this article can be accessed online at https://doi.org/10.1080/17588928.2026.2665610

Previously, it was hypothesized that interactions between the large-scale brain networks involved in attention and mind wandering are manifest in the electrophysiological dynamics of electroencephalographic (EEG) microstates (Zanesco et al., 2021). EEG microstates preserve information about global brain network activity while offering the temporal precision needed to track fast changes in attentional state. Distinct microstate topographies have been proposed to reflect brief configurations of activity across distributed networks of neural generators, with transitions between microstates indexing sequential patterns of connectivity between networks over time (Khanna et al., 2015; Zanesco, 2024). EEG microstates therefore provide a promising approach for examining the rapid dynamics of attentional fluctuations, capturing transient, quasi-stable topographical patterns of scalp voltage that last approximately 30–120 ms (Michel & Koenig, 2018).

The microstate approach differs from traditional EEG methods such as event-related potentials and spectral power analyses (e.g., quantifying alpha power), which typically focus on time-locked or frequency-specific activity within restricted regions. These traditional approaches provide limited information about how large-scale neural configurations evolve over time and therefore cannot fully capture rapid, time-varying transitions in brain states during ongoing task performance (Zanesco et al., 2021). In contrast, EEG microstate analysis characterizes brief, quasi-stable topographical patterns that reflect discrete global brain states and their moment-to-moment transitions at a millisecond timescale.

Canonical microstates can be clustered into a small set of recurring topographical configurations (typically labeled A – E), each associated with distinct patterns of large-scale functional activity (Koenig et al., 2024; Zanesco, 2024). Of particular relevance to sustained attention, microstate C has been linked based on initial source localization studies to activity in regions of the default mode network (Brechet et al., 2019; Custo et al., 2017; Tarailis et al., 2025; Valt et al., 2024; Zanesco et al., 2026), which is typically engaged during internally oriented cognitive processing, such as during mind wandering (Christoff et al., 2009; Hasenkamp et al., 2012). In contrast, microstate E has been less consistently investigated. At least one study has associated microstate E with regions in the salience and cingulo-opercular networks (Custo et al., 2017), which are implicated in maintaining tonic alertness and coordinating switching between networks involved in goal-directed externally-focused attention and the default mode network (Goulden et al., 2014; Hasenkamp et al., 2012; Sadaghiani & D'Esposito, 2015). However, other work has linked microstates D and E to attention and cognitive control processes associated with the frontoparietal and dorsal attention networks (DiMuccio et al., 2023; Ngo et al., 2026; Tarailis et al., 2024). These varying interpretations highlight that further work is needed to clarify the neural generators and functional significance of individual EEG microstates.

Nevertheless, a prior study involving experience sampling during completion of a sustained attention task, the Sustained Attention to Response Task (SART; Robertson et al., 1997), found that microstate C was more prominent during episodes of self-reported mind wandering, whereas microstate E was more prominent during self-reported on-task states (Zanesco et al., 2021). Similarly, greater response time variability was accompanied by increased prominence of microstate C. Behavioral studies of sustained attention and mind wandering have also frequently reported that increased response time variability, often operationalized as the intraindividual coefficient of variation (RT ICV), increases with greater time-on-task (McVay & Kane, 2009; Schwartzman et al., 2025; Zanesco et al., 2024), is associated with states of mind wandering, and is widely considered a sensitive behavioral marker of attentional instability (Esterman et al., 2013; Kofler et al., 2013; Unsworth, 2015). Together, these findings suggest that the relative prominence of microstates C and E may differentiate modes of cognition characterized by off-task, internally focused processing versus on-task, externally focused engagement.

Given recent work characterizing robust increases in rates of mind wandering with greater time-on-task (i.e., Schwartzman et al., 2025; Zanesco et al., 2024, 2025), it is critical to examine whether the prominence and dynamics of specific microstates also change in line with these shifts in attentional focus. To date, no studies have examined whether EEG microstates exhibit systematic time-on-task effects during sustained attention. To investigate the time course of microstates during task performance, we conducted secondary analyses of the data discussed above and originally reported by Zanesco et al. (2021), which entailed participants completing a 45-min version of the SART. Accordingly, our primary hypotheses focused on microstates C and E based on prior findings from this dataset linking these microstates to mind wandering and on-task states during sustained attention (Zanesco et al., 2021). Analyses of the remaining canonical microstates (A, B, and D) are reported in the Supplementary Materials.

We used growth curve modeling of experience-sampling reports and behavioral performance to confirm predicted patterns of increasing mind wandering and declining task performance with greater time-on-

task. Next, growth curve modeling was applied to the EEG microstate metrics, derived from the pre-stimulus periods of trials preceding mind wandering probes, to examine how microstate dynamics changed with greater time-on-task. Guided by prior analyses of this dataset linking microstate C to mind wandering and microstate E to on-task focus (Zanesco et al., 2021), we hypothesized that microstate C metrics (global explained variance, global field power, duration, occurrence, and time coverage) would increase with greater time-on-task, whereas the corresponding microstate E metrics would decrease.

Method

Participants

Thirty-six undergraduate students (18 females, *M* age = 18.83 years, *SD* age = 1.28, age range = 18–25) participated in this study. No participants reported a history of neurological disorders or head injury with loss of consciousness, and all had normal or corrected-to-normal vision. The study was approved by the Institutional Review Board of the University of Miami and participants provided written informed consent and received course credit for their participation. Data from two participants were excluded from analyses: one for incomplete data, and one for poor performance (more than 4 *SD* below the group accuracy mean); resulting in a final sample of 34.

Procedure

Participants completed a modified version of the Sustained Attention to Response Task (Robertson et al., 1997) with face stimuli (F-SART) in a sound-attenuating booth, while 64-channel EEG were recorded.

Sustained attention to response task with faces (F-SART)

A summary of the F-SART is provided below and is described in detail by Denkova et al. (2018) and Zanesco et al. (2021). F-SART consisted of 833 upright faces (non-targets) and 45 upside-down faces (targets) presented in a pseudorandom order one at a time in the center of the screen for 500 msec and followed by a fixation cross of variable duration (*M* = 1,487 msec, *SD* = 115, range: 1,313–1,693). Participants were instructed to respond via button press to the non-targets and withhold their response to the targets. Intermittently during the task, 45 experience sampling mind wandering probes included two questions that were presented for 4,000 msec each. The first question asked, 'Where was your attention focused just before the probe?' and participants responded by selecting either (1) 'on-task' or (2) 'off-task.' Participants were instructed that 'on-task' meant their attention was focused completely on task performance, whereas 'off-task' referred to attention directed toward something unrelated to the task, such as task-unrelated thoughts. The second question asked, 'How confident are you in your previous answer?' and participants responded by selecting either (1) low, (2) medium, or (3) high. The second question was not examined as part of the present analyses.

The occurrence of target and probes trials was pseudorandomized in trial order with the restriction that there were at least six consecutive non-target trials before target or probe trials and the average interval between probe trials was ~50 s (range = 12–83 seconds). This enabled the examination of pre-stimulus brain dynamics during the seconds leading up to the probe. Each participant received the same trial ordering. See Figure 1 for a schematic depicting several trials of the F-SART.

The primary dependent variables from the F-SART were responses to mind wandering probes (on- or off-task), intra-individual coefficient of variation (ICV) in response times (RT), and accuracy as measured by *A'*. RT ICV reflects trial-to-trial variability in response speed and was calculated as the standard deviation of RTs divided by their mean RT. *A'* (Stanislaw & Todorov, 1999) is an accuracy-based nonparametric measure of sensitivity based on a composite of the number of correct hits (correctly withholding a response to target trials) and false alarms (incorrectly withholding a response to non-target trials).

Whereas previous analyses of this dataset focused on overall mind wandering and performance effects (Denkova et al., 2018; Zanesco et al., 2021), the present study examined how these measures changed as a function of time-on-task. To assess changes in mind wandering with greater time-on-task, probe responses were coded such that higher values reflected greater off-task responding (on-task = 0, off-task = 1), allowing for the characterization of changes in mind wandering across sequential probe trials. To assess changes in RT ICV with greater time-on-task, values were computed for the six non-target trials preceding each probe trial, allowing for the characterization of changes in RT ICV across sequential probe trials. To assess changes in *A'* with greater time-on-task, *A'* was calculated separately for three consecutive blocks of trials. Each block contained 15 target trials and 266, 279, and 288 non-target trials, respectively.

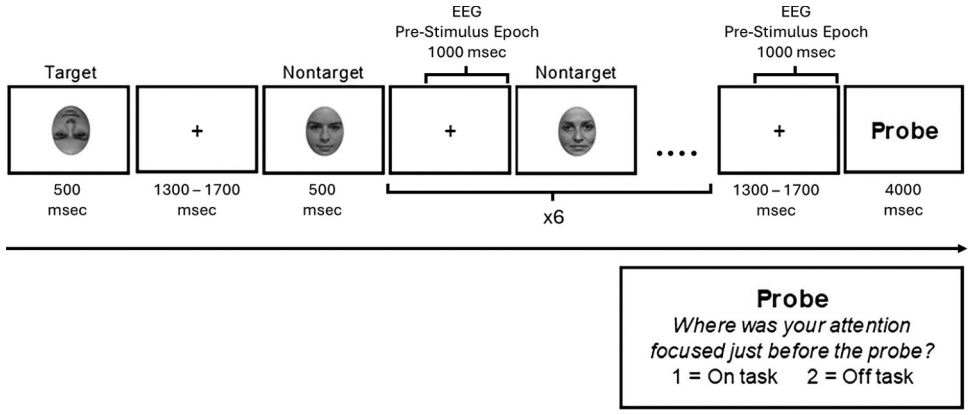

Figure 1. Schematic representation of F-SART trials. Note. Participants were instructed to respond via button press to frequently occurring upright faces (non-targets) and withhold responses to infrequently occurring inverted faces (targets). They were also instructed to answer an experience sampling probe question that intermittently appeared, assessing if their attention was "on-task" or "off-task." At least six non-target trials always preceded probes. Pre-stimulus epochs of these six trials and the pre-stimulus epoch of the probe were included in EEG analyses.

EEG data acquisition and processing

EEG acquisition and processing were previously described by Zanesco et al. (2021) and are repeated in brief here. EEG was recorded from 64 Ag/AgCl electrodes located according to the 10–20 International System (American Electroencephalographic Society, 1991) using a BioSemi ActiveTwo system. Data were acquired at a sampling rate of 256 Hz, bandpass filtered online at 0.16–100 Hz, and subsequently processed offline using the free Cartool software toolbox version 3.7 (Brunet et al., 2011). Recordings were referenced to a common average of all 64 scalp electrodes and were bandpass filtered between 1 and 40 Hz (zero-phase, 12 dB/octave). EEG epochs were visually inspected for artifacts, and segments containing eye blinks, eye movements, or excessive noise were removed. Channels with intermittent connectivity or periods of extreme amplitude were interpolated using 3D spherical spline interpolation. EEG was downsampled to 128 Hz using cascaded integrator-comb and high pass finite impulse response filters in Cartool.

The EEG data before each probe trial were then segmented into seven 1,000 msec pre-stimulus epochs – the time immediately preceding the six non-target trials leading up to the probe (270 total across the task) and one 1,000 msec epoch immediately preceding the probe itself (45 total across the task). Pre-stimulus epochs therefore began roughly 800 to 1,200 msec after the presentation of the previous face stimulus. See Figure 1 for a schematic depicting the EEG pre-stimulus epochs. Epochs were included regardless of accuracy (i.e., correct and incorrect non-targets). Each epoch was visually screened and removed if ocular movements, eyeblinks, excessive myographic noise, or other artifacts occurred within the window. On average, 213.9 (SD = 43.8, range = 116–274) pre-stimulus epochs of EEG were included in analyses after screening. Finally, EEG was spatially smoothed using the spatial interseptile weighted mean (Michel & Brunet, 2019).

Topographic segmentation and microstate estimation

EEG microstate clustering and segmentation methods were previously reported by Zanesco et al. (2021) and are repeated in brief here. An adapted k-means clustering method was used to determine the optimal number of topographic clusters (k) that explain the topographic microstate configurations present in the EEG. Clustering was implemented in Cartool (Brunet et al., 2011) in two stages. Voltage maps were first generated at local maxima (peaks) in the global field power (GFP; Skrandies, 1990) from the time series of contiguous epochs for each individual. Voltage maps were assigned to clusters based on their spatial correlations using k-means clustering, creating k clusters of maps for each individual. Maps were only assigned to a cluster if the spatial correlation with the centroid map exceeded 0.5. Spatial correlations are based on the relative topographical configuration between maps but not the polarity by ignoring the sign of the correlation coefficients (Michel et al., 2009).

A second k-means clustering step determined the optimal cluster centroids summarizing all the subject-level cluster results. This was done to identify the optimal global clusters that best explain the subject-level cluster centroids across all participants. The optimal number of k global clusters for this procedure was determined using a clustering selection metacriterion (see Brechet et al.,

2019; Custo et al., 2017), resulting in a set of *k* global centroids that best represent the topographic configurations of all participants. This resulted in five global clusters of microstate topographies that together explained 87.51% of the global explained variance (GEV) among the individual subject cluster centroids. These five global clusters (A – E) were selected as the optimal number based on the optimization metacriterion and appeared to be a good representation of the most common topographic patterns observed among all participants.

Microstate labeling and parameterization

The global cluster centroids, representing the most common topographic configurations of microstates present in the EEG, were used to label the original pre-stimulus epochs to generate time series of microstate sequences. Voltage maps at each EEG sample were labeled according to the global cluster centroid with which it had the highest spatial correlation. Samples exhibiting low spatial correlations with all centroids (i.e., <0.5) were excluded from classification. Polarity was ignored during labeling: the sign of the spatial correlation was corrected during assignment. Temporal smoothing was subsequently applied to the resulting microstate sequences by ignoring microstate segments lasting fewer than three consecutive samples (i.e., ≤23 ms). The time points from these short segments were reallocated to the preceding and following microstates in the sequence. The time series samples of all 7274 pre-stimulus epochs were labeled. On average, 86.67% (*SD* = 10.2%, range = 13–100%) of samples within a pre-stimulus epoch were successfully labeled (i.e., spatial correlation >0.5). The five global microstate topographies explained 62.11% (*SD* = 7.5%, range = 29.3–-88.1%) of the GEV on average.

Several measures describing the strength and temporal dynamics of microstates were subsequently derived from the labeled microstate time series of each pre-stimulus epoch. These measures included the *global explained variance* (GEV), *mean global field power* of GFP maxima, mean *microstate duration* (in msec), *frequency of occurrence* (in Hz), and percent time *coverage*. See Figure 2 for a schematic depicting the calculation of microstate measures. These measures are described in more detail in Zanesco et al. (2021).

Whereas previous analyses of this dataset focused on how microstate measures were related to on- vs. off-task probe reports (Zanesco et al., 2021), the present study focused on how microstate measures change with greater time-on-task. To do so, microstate measures were averaged across the set of consecutive pre-stimulus epochs preceding each probe (up to 7 pre-stimulus epochs per probe), allowing characterization of changes in microstates across sequential probe trials – consistent with the approach used for mind wandering and RT ICV.

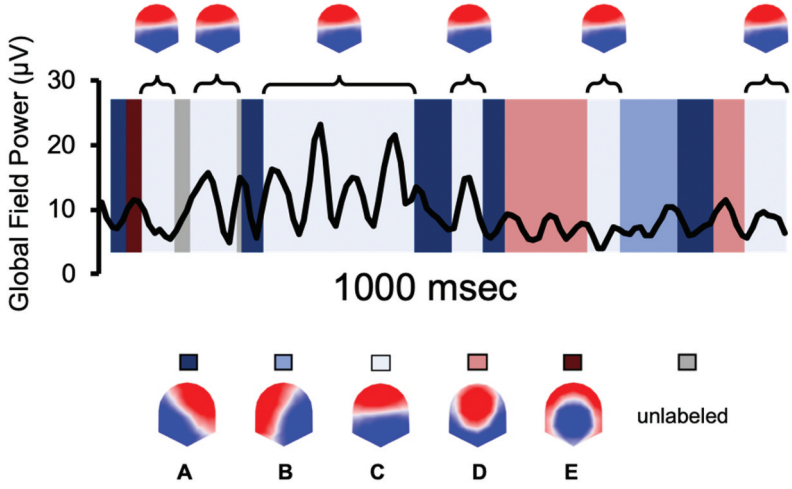

Figure 2. Calculation of microstate measures for a single 1000-msec pre-stimulus epoch. Note. Schematic illustrating the calculation of measures from the microstate time series for a single 1000-msec epoch. Global explained variance (GEV %), mean global field power (GFP) of GFP peaks (μV), mean duration (in msec), occurrence rate (in times per second, Hz), and percent time coverage (%) are calculated for each microstate configuration. The time series of microstates is shown with the GFP overlaid on top and the duration and occurrence of Microstate C visualized above. Microstate C explained 54.6% of the GEV for this epoch, occurred six times, had a mean duration of 68.4 msec when it occurred, and covered 49.6% of the epoch. The mean GFP at the GFP peaks was 13.4 μV for Microstate C. For each probe, these measures are averaged with the other epochs preceding the probe to create a set of probe-averaged microstate measures.

Analyses

Growth curve models were used to estimate rates of linear change in self-reported mind wandering probe responses (on-task vs. off-task), behavioral performance (RT ICV and *A'*), and measures of microstate dynamics, as a function of time-on-task. All growth curve models were estimated with maximum likelihood in the mixed-effects modeling framework (McNeish & Matta, 2018) using SAS Version 9.4, and the significance of fixed and random effects parameter estimates were evaluated. Growth curve models estimated parameters describing a starting point (i.e., intercept) and linear rate of change (i.e., slope) in outcome variables as a function of time-on-task. Fixed and random effects of sequential probe trial were included in the growth curve models of mind wandering, RT ICV, and EEG microstates to describe linear rates of change across sequential probe trials. For models of mind wandering probe ratings (i.e., 0 = on-task and 1 = off-task), generalized linear mixed-effects models were used to estimate the log-odds of an off-task response, included a logit link function, and utilized maximum likelihood estimation with adaptive quadrature. Because calculating *A'* requires aggregating hits and false-alarms from target and non-target trials, task block was used to characterize changes with greater time-on-task instead of sequential probe trials. Therefore, fixed and random effects of block were included in the growth curve model of *A'*.

Results

Mind wandering and behavioral performance as a function of time-on-task

Growth curve models were used to test whether self-reported mind wandering and behavioral performance in the SART exhibited the expected pattern of increasing off-task thoughts and declining performance with greater time-on-task. The odds of reporting being off-task linearly increased over sequential probes, such that individuals were 1.032 times more likely to report being off-task for each successive probe ($b = 0.0313$ log-odds ratio, $SE = 0.0059$, $p < .001$, 95% CI [0.0193, 0.0433]). The odds of being off-task (vs. on-task) were 0.242 ($b = -1.4198$ log-odds, $SE = 0.3550$, 95% CI [−2.1422, −0.6975]) at the first probe. RT ICV increased linearly with each sequential probe trial by 0.0022 units ($SE = 0.0006$, $p < .001$, 95% CI [0.0010, 0.0034]) from the intercept of 0.1778 at the first probe trial ($SE = 0.0097$, 95% CI [0.1582, 0.1975]). *A'* decreased linearly each block by −0.0259 units ($SE = 0.0072$, $p = .001$, 95% CI [−0.0406, −0.0113]) from the intercept of 0.9033 at the first block ($SE = 0.0078$, 95% CI [0.8857, 0.9190]). These findings confirm the expected pattern of increasing likelihood individuals report being off-task, increasing response time variability, and declining accuracy with greater time-on-task. See Figures 3(a–c) for plots of model results.

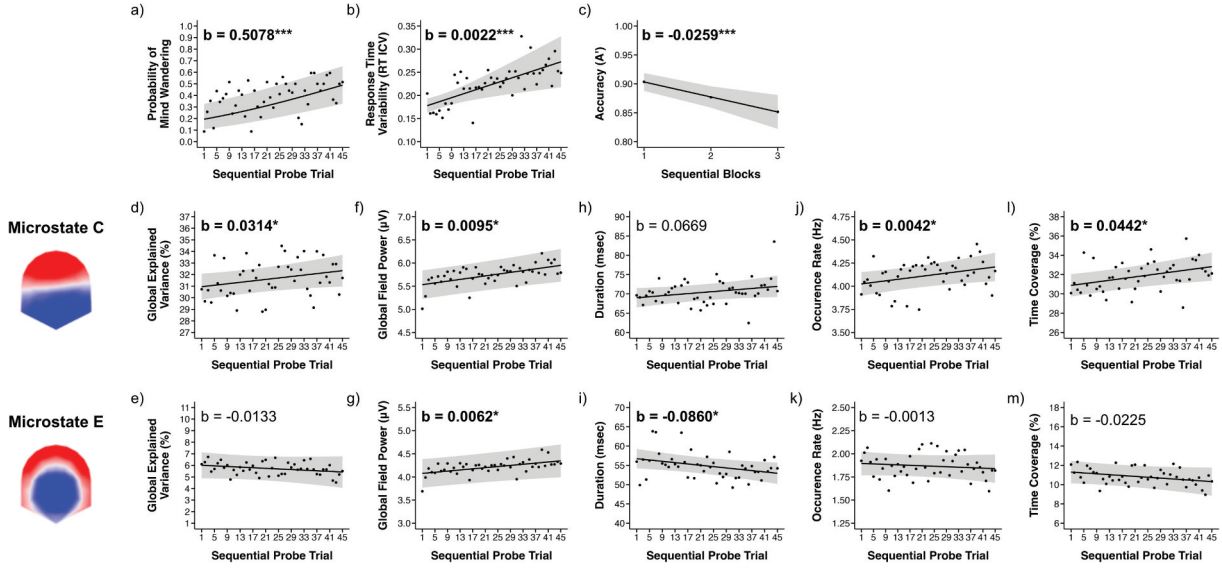

Figure 3. Growth curve models of self-reported mind wandering, behavioral, and microstate measures. Note. Estimated trend lines and observed means for (a) probability of responding off-task (mind wandering), (b) response time variability (RT ICV), (c) accuracy (*A'*), and d—m) microstates C and E measures. Error ribbons around trend lines represent model estimated 95% confidence intervals. Slope estimate values, *b*, are also provided. Bold estimates represent statistically significant slopes at *$p < .05$, **$p < .01$, ***$p < .001$. $N = 34$.

Table 1. Parameter estimates from analyses of microstate measures as a function of time-on-task.

Estimate	GEV	GFP	Duration	Occurrence	Coverage
Fixed Effects					
Intercept (Microstate C)	30.954 (0.575)***	5.523 (0.1575)***	68.999 (1.287)***	4.024 (0.066)***	30.881 (0.596)***
Microstate E	−24.946 (0.486)***	−1.452 (0.0547)***	−12.266 (1.174)***	−2.129 (0.059)***	−19.578 (0.509)***
Slope (Microstate C)	0.031 (0.016)*	0.010 (0.003)***	0.067 (0.038)	0.004 (0.002)*	0.044 (0.016)**
Slope × Microstate E	−0.045 (0.019)*	−0.003 (0.002)	−0.153 (0.046)***	−0.005 (0.002)*	−0.067 (0.020)***
Random Effects					
Intercept Variance	7.228 (2.239)	0.792 (0.198)	32.877 (10.891)	0.086 (0.028)	7.680 (2.393)
Covariance	0.014 (0.039)	−0.0002 (0.002)	−0.132 (0.220)	0.0003 (0.0005)	0.039 (0.039)
Slope Variance	0.002 (0.001)	0.0001 (0.00004)	0.012 (0.007)	0.00002 (0.00002)	0.002 (0.001)
Residual Variance	46.078 (1.200)	0.546 (0.014)	268.78 (7.025)	0.690 (0.018)	50.559 (1.316)
Obs.	3018	2018	2996	3018	3018
N	34	34	34	34	34

Note: Maximum likelihood estimates are reported from mixed effects models of GEV (%), GFP (in μV), microstate duration (in msec), per-second rate (*Hz*) of microstate occurrence, and percent time coverage (%) for fixed effects of microstate configuration (Microstates C and E) and sequential probe number. Microstate C serves as the reference. The number of participants (*N*) and observations contributing to the analyses are provided. Standard errors are reported in parentheses. Significance is provided for fixed effects estimates. *$p < .05$. **$p < .01$. ***$p < .001$.

Microstate dynamics as a function of time-on-task

See Table 1 for model parameter estimates of each microstate measure.

Global explained variance (GEV)

We first examined the mean global explained topographic variance (GEV) of microstates C and E as a function of sequential probes. We found no significant main effect of sequential probe, $F(1, 34) = 0.54$, $p = .463$, but a significant interaction between microstate configuration and sequential probe, $F(1, 2950) = 5.53$, $p = .019$, such that the microstates showed significantly different patterns of change ($b = -0.0447$, $SE = 0.0190$, $p = .019$, 95% CI [−0.0820, −0.0074]). While microstate C linearly increased in GEV with each sequential probe by 0.0314 ($SE = 0.0156$, $p = .047$, 95% CI [0.0004, 0.0624]) from the intercept of 30.9539 at the first probe trial ($SE = 0.5749$, 95% CI [29.7993, 32.1084]), microstate E showed no significant change over sequential probes ($b = -0.0133$, $SE = 0.0156$, $p = .397$, 95% CI [−0.0443, 0.0177]). See Figures 3(d–e) for plots of model results.

Global field power (GFP)

We examined the mean global field power (GFP in μV) of microstates C and E as a function of sequential probes. We found a significant main effect of sequential probe, $F(1, 34.1) = 11.74$, $p = .002$, but no significant interaction between microstate configuration and sequential probe, $F(1, 2950) = 2.59$, $p = .108$. As such, these microstates linearly increased in amplitude on each sequential probe by 0.0078 μV ($SE = 0.0023$, $p = .002$, 95% CI [0.0032, 0.0125]). Examination of the trends for separate microstates demonstrated that microstate C linearly increased in amplitude on each sequential probe by 0.0095 μV ($SE = 0.0025$, $p < .001$, 95% CI [0.0046, 0.0145]), and microstate E linearly increased in amplitude on each sequential probe by 0.0062 μV ($SE = 0.0025$, $p = .018$, 95% CI [0.0011, 0.0112]). See Figures 3 (f–g) for plots of model results.

Duration

We examined the mean duration (in msec) of microstates C and E as a function of sequential probes. We found no significant main effect of sequential probe, $F(1, 34.1) = 0.10$, $p = .749$, but a significant interaction between microstate configuration and sequential probe, $F(1, 2929) = 10.98$, $p < .001$. Microstate C did not significantly increase in duration with each sequential probe ($b = 0.0669$, $SE = 0.0375$, $p = .078$, 95% CI [−0.0077, 0.1414]) from the intercept of 68.9993 at the first probe trial ($SE = 1.2865$, 95% CI [66.4193, 71.5793]). In contrast, microstate E demonstrated a significantly different pattern of change ($b = -0.1529$, $SE = 0.0461$, $p < .001$, 95% CI [−0.2433, −0.0624]), such that microstate E significantly decreased in duration over sequential probes ($b = -0.0860$, $SE = 0.0377$, $p = .025$, 95% CI [−0.1609, −0.0111]). See Figures 3(h–i) for plots of model results.

Occurrence

We examined the mean occurrence rate (in *Hz*) of microstates C and E as a function of sequential probes. We found no significant main effect of sequential probe, $F(1, 33.8) = 1.10$, $p = .301$, but a significant interaction between microstate configuration and sequential probe, $F(1, 2950) = 5.46$, $p = .020$. Microstate C linearly increased in rate of occurrence on each sequential probe by 0.0042 *Hz* ($SE = 0.0018$, $p = .023$, 95% CI [0.0006, 0.0077]) from the intercept of 4.024 *Hz* at the first probe trial ($SE = 0.0655$, 95% CI [3.8928, 4.1555]). In contrast, microstate E demonstrated a significantly different pattern of change ($b = -0.0054$ *Hz*, $SE = 0.0023$, $p = .020$, 95% CI [−0.0100, −0.0009]), such that microstate

E showed no significant change over sequential probes ($b = -0.0013$ *Hz*, $SE = 0.0018$, $p = .481$, 95% CI [−0.0049, 0.0023]). See Figures 3(j–k) for plots of model results.

Coverage

We finally examined the mean percentage time coverage of microstates C and E as a function of sequential probes. We found no significant main effect of sequential probe, $F(1, 34.3) = 0.78$, $p = .384$, but a significant interaction between microstate configuration and sequential probe, $F(1, 2950) = 11.18$, $p < .001$. Microstate C linearly increased in percentage time coverage on each sequential probe by 0.0442 ($SE = 0.0158$, $p = .006$, 95% CI [0.0127, 0.0756]) from the intercept of 30.8806 at the first probe trial ($SE = 0.5961$, 95% CI [29.6839, 32.0772]). In contrast, microstate E demonstrated a significantly different pattern of change ($b = -0.0666$, $SE = 0.0199$, $p < .001$, 95% CI [−0.1057, −0.0275]), such that microstate E showed no significant change over sequential probes ($b = -0.0225$, $SE = 0.0158$, $p = .159$, 95% CI [−0.0539, 0.0090]). See Figures 3(l–m) for plots of model results.

Additional microstates

Although our hypotheses focused on microstates C and E, we also examined time-on-task effects for the remaining microstates (A, B, and D). Growth curve analyses of the same microstate metrics (GEV, GFP, duration, occurrence, and time coverage) revealed that while GFP increased with time-on-task across all microstates, none of these microstates exhibited systematic changes in GEV, duration, occurrence, or time coverage. Detailed model results for microstates A, B, and D are provided in the Supplementary Materials.

Discussion

The present study examined mind wandering, behavioral, and neural patterns over a 45-min version of the Sustained Attention to Response Task (SART). Consistent with established time-on-task effects in numerous studies (see Zanesco et al., 2024), the likelihood of reporting off-task thoughts (mind wandering) increased, response time variability (RT ICV) increased, and accuracy (*A'*) decreased with greater time-on-task. EEG microstate analyses revealed a corresponding pattern in neural activity: microstate C, linked to internally oriented task-unrelated thought (Zanesco et al., 2021), became increasingly dominant (greater occurrence and time coverage) with greater time-on-task, whereas microstate E, associated with on-task focus (Zanesco et al., 2021), declined in duration. Together, these results suggest that EEG microstate state dynamics closely resemble time-on-task changes in mind wandering and sustained attention, reflecting a shift from externally oriented task focus toward internally oriented, mind wandering states.

The opposing trajectories of microstates C and E point to a gradual reorganization of large-scale neural dynamics with greater time-on-task. It is important to note that EEG microstates represent brief, transient configurations of large-scale brain activity, typically lasting tens of milliseconds before transitioning to another configuration. These millisecond microstate dynamics highlight the general principle that cognition depends on rapid switching among brain states dependent on distinct neuronal networks. Consequently, shifts in the prevalence of specific microstates can dramatically shift the overall trajectory of sequential states through which the brain continuously traverses.

One interpretation is that these dynamics reflect changes in overall task engagement, with microstate C becoming more prominent as attention disengages from the task and microstate E diminishing as task engagement wanes. This view is consistent with prior work linking microstate C to off-task states, and microstate E to on-task focus during sustained attention tasks (Zanesco et al., 2021). At the same time, these patterns may also reflect shifts in attentional orientation from externally directed task processing toward internally oriented cognition, a distinction commonly used to characterize different forms of attention (Chun et al., 2011; Hadash et al., 2025). Consistent with this interpretation, prior work has localized microstate C to regions overlapping with the default mode network and internally-oriented cognition (Custo et al., 2017) and microstate E has been proposed to reflect neural configurations supporting externally oriented task processing, with some studies localizing it to task-relevant attention, control, or salience-related regions (Brechet et al., 2019; Custo et al., 2017; Ngo et al., 2026; Zanesco et al., 2026). However, the neural generators of EEG microstates remain an active area of investigation, and these correspondences should be considered tentative.

Overall, these findings suggest that time-on-task effects reflect overlapping shifts in task engagement and attentional orientation. As task performance unfolds, neural configurations supporting external attentional control diminish, while those associated with internally generated thought become more prevalent. Therefore, rather than reflecting a simple depletion of cognitive resources (Grier et al., 2003; Warm et al., 2008), this pattern aligns with accounts proposing that attentional failures arise from competitive interactions among large-scale networks, wherein control-related systems disengage as

default-mode processes, such as mind wandering, become increasingly dominant over time (Thomson et al., 2015).

These findings identify microstate dynamics as sensitive markers of sustained attention. As such, the EEG microstate approach provides a temporally precise means for tracking rapid large-scale neural transitions that accompany fluctuations of attention. However, several limitations should be acknowledged. First, while the current analyses reveal systematic time-on-task changes in microstate properties, the scalp-recorded topographies cannot directly resolve the underlying neural generators or determine causal interactions among large-scale networks. Second, time-on-task effects were more robust for microstate C than for microstate E, emerging across four of the five metrics examined for microstate C but only one for microstate E. One possibility is that microstate C more closely tracks gradual shifts in bias toward internally oriented cognition during sustained task performance. However, given the relatively modest effects observed for microstate E, this limits the strength of inferences that can be drawn regarding the functional role of microstate E in time-on-task effects. Moreover, prior studies have reported somewhat varying source localization patterns for individual microstates (Custo et al., 2017; Tarailis et al., 2024), further underscoring the need for caution when attributing specific functional networks to particular scalp topographies. Other canonical microstates have also been linked to attention and cognition. For example, microstate D has been associated with attention and cognitive control processes of the dorsal attention network (Tarailis et al., 2024). However, we did not observe systematic time-on-task effects for microstate D (or microstates A and B) in the present data (see Supplemental Materials).

Future work combining microstate analyses with continuous physiological indices (e.g., pupil diameter, heart-rate variability) or neuroimaging could clarify how neural, attentional, and arousal processes jointly evolve during sustained performance. This approach may be particularly valuable for evaluating how interventions that target attentional stability – such as mindfulness training (Jha et al., 2025; Price et al., 2023; Zainal & Newman, 2024) – shape the temporal coordination of large-scale neural networks. Overall, the present findings demonstrate that EEG microstates exhibit systematic time-on-task changes that resemble behavioral and experiential markers of attentional decline, revealing how the large-scale organization of brain activity gradually reconfigures as attention drifts from external task demands toward internally oriented thought.

Acknowledgments

We utilized the freely available Cartool software toolbox (cartoolcommunity.unige.ch) programmed by Denis Brunet from the Functional Brain Mapping Laboratory, Geneva, Switzerland and supported by the Center for Biomedical Imaging of Geneva and Lausanne.

Disclosure statement

No potential conflict of interest was reported by the author(s).

Funding

The author(s) reported that there is no funding associated with the work featured in this article.

ORCID

Jason S. Tsukahara http://orcid.org/0000-0003-3570-1977

References

Brechet, L., Brunet, D., Birot, G., Gruetter, R., Michel, C. M., & Jorge, J. (2019). Capturing the spatiotemporal dynamics of self-generated, task-initiated thoughts with EEG and fMRI. *Neuroimage*, *194*, 82–92. https://doi.org/10.1016/j.neuroimage.2019.03.029

Brunet, D., Murray, M. M., & Michel, C. M. (2011). Spatiotemporal analysis of multichannel EEG: CARTOOL. *Computational Intelligence and Neuroscience*, *2011*, 813870. https://doi.org/10.1155/2011/813870

Christoff, K., Gordon, A. M., Smallwood, J., Smith, R., & Schooler, J. W. (2009). Experience sampling during fMRI reveals default network and executive system contributions to mind wandering. *Proceedings of the National Academy of Sciences*, *106*(21), 8719–8724. https://doi.org/10.1073/pnas.0900234106

Chun, M. M., Golomb, J. D., & Turk-Browne, N. B. (2011). A taxonomy of external and internal attention. *Annual Review of Psychology*, *62*, 73–101. https://doi.org/10.1146/annurev.psych.093008.100427

Custo, A., Van De Ville, D., Wells, W. M., Tomescu, M. I., Brunet, D., & Michel, C. M. (2017). Electroencephalographic resting-state networks: Source localization of microstates. *Brain Connectivity*, *7*(10), 671–682. https://doi.org/10.1089/brain.2016.0476

Denkova, E., Brudner, E. G., Zayan, K., Dunn, J., & Jha, A. P. (2018). Attenuated face processing during mind wandering. *Journal of Cognitive Neuroscience*, *30*(11), 1691–1703. https://doi.org/10.1162/jocn_a_01312

DiMuccio, F., Simonet, M., Brandner, C., Ruggeri, P., & Barral, J. (2023). Cardiorespiratory fitness modulates prestimulus EEG microstates during a sustained attention task. *Frontiers in Neuroscience*, *17*, 1188695. https://doi.org/10.3389/fnins.2023.1188695

Esterman, M., Noonan, S. K., Rosenberg, M., & Degutis, J. (2013). In the zone or zoning out? Tracking behavioral and neural

fluctuations during sustained attention. *Cerebral Cortex*, *23* (11), 2712–2723. https://doi.org/10.1093/cercor/bhs261

Esterman, M., & Rothlein, D. (2019). Models of sustained attention. *Current Opinion in Psychology*, *29*, 174–180. https://doi.org/10.1016/j.copsyc.2019.03.005

Fox, K. C., Spreng, R. N., Ellamil, M., Andrews-Hanna, J. R., & Christoff, K. (2015). The wandering brain: Meta-analysis of functional neuroimaging studies of mind-wandering and related spontaneous thought processes. *Neuroimage*, *111*, 611–621. https://doi.org/10.1016/j.neuroimage.2015.02.039

Goulden, N., Khusnulina, A., Davis, N. J., Bracewell, R. M., Bokde, A. L., McNulty, J. P., & Mullins, P. G. (2014). The salience network is responsible for switching between the default mode network and the central executive network: Replication from DCM. *Neuroimage*, *99*, 180–190. https://doi.org/10.1016/j.neuroimage.2014.05.052

Grier, R. A., Warm, J. S., Dember, W. M., Matthews, G., Galinsky, T. L., Szalma, J. L., & Parasuraman, R. (2003). The vigilance decrement reflects limitations in effortful attention, not mindlessness. *Human Factors*, *45*(3), 349–359.

Hadash, Y., Dar, O., Amir, I., Braver, T. S., & Bernstein, A. (2025). The mindfulness internal attention (MIA) framework: Uncovering the attentional mechanisms of mindfulness training. *Annual Review of Psychology*, *77*(1).1.1–.1.29. https://doi.org/10.1146/annurev-psych-012925-030843

Hasenkamp, W., Wilson-Mendenhall, C. D., Duncan, E., & Barsalou, L. W. (2012). Mind wandering and attention during focused meditation: A fine-grained temporal analysis of fluctuating cognitive states. *Neuroimage*, *59*(1), 750–760. https://doi.org/10.1016/j.neuroimage.2011.07.008

Jha, A. P., Izaguirre, M. K., & Adler, A. B. (2025). Mindfulness training in military settings: Emerging evidence and best-practice guidance. *Current Psychiatry Reports*, *27*, 393–407. https://doi.org/10.1007/s11920-025-01608-6

Khanna, A., Pascual-Leone, A., Michel, C. M., & Farzan, F. (2015). Microstates in resting-state EEG: Current status and future directions. *Neuroscience and Biobehavioral Reviews*, *49*, 105–113. https://doi.org/10.1016/j.neubiorev.2014.12.010

Koenig, T., Diezig, S., Kalburgi, S. N., Antonova, E., Artoni, F., Brechet, L., Britz, J., Croce, P., Custo, A., Damborska, A., Deolindo, C., Heinrichs, M., Kleinert, T., Liang, Z., Murphy, M. M., Nash, K., Nehaniv, C., Schiller, B. Smailovic, U. . . . Zou, Q. (2024). Eeg-meta-microstates: Towards a more objective use of resting-state eeg microstate findings across studies. *Brain Topography*, *37*(2), 218–231. https://doi.org/10.1007/s10548-023-00993-6

Kofler, M. J., Rapport, M. D., Sarver, D. E., Raiker, J. S., Orban, S. A., Friedman, L. M., & Kolomeyer, E. G. (2013). Reaction time variability in ADHD: A meta-analytic review of 319 studies. *Clinical Psychology Review*, *33*, 795–811. https://doi.org/10.1016/j.cpr.2013.06.001

Margulies, D. S., Ghosh, S. S., Goulas, A., Falkiewicz, M., Huntenburg, J. M., Langs, G., Bezgin, G., Eickhoff, S. B., Castellanos, F. X., Petrides, M., Jefferies, E., & Smallwood, J. (2016). Situating the default-mode network along a principal gradient of macroscale cortical organization. *Proceedings of the National Academy of Sciences*, *113*(44), 12574–12579. https://doi.org/10.1073/pnas.1608282113

McNeish, D., & Matta, T. (2018). Differentiating between mixed-effects and latent-curve approaches to growth modeling. *Behavior Research Methods*, *50*(4), 1398–1414. https://doi.org/10.3758/s13428-017-0976-5

McVay, J. C., & Kane, M. J. (2009). Conducting the train of thought: Working memory capacity, goal neglect, and mind wandering in an executive-control task. *Journal of Experimental Psychology: Learning, Memory & Cognition*, *35* (1), 196–204. https://doi.org/10.1037/a0014104

Michel, C. M., & Brunet, D. (2019). Eeg source imaging: A practical review of the analysis steps. *Frontiers in Neurology*, *10*, 325. https://doi.org/10.3389/fneur.2019.00325

Michel, C. M., & Koenig, T. (2018). Eeg microstates as a tool for studying the temporal dynamics of whole-brain neuronal networks: A review. *Neuroimage*, *180*, 577–593. https://doi.org/10.1016/j.neuroimage.2017.11.062

Michel, C. M., Koenig, T., Brandeis, D., Gianotti, L. R., & Wackermann, J. (2009). *Electrical neuroimaging*. Cambridge University Press.

Ngo, C., Bek, E., Stasytyte, M., Newman, L. A., Elizalde, R., Kanthi, A., Manjunath, N. K., & Michel, C. M. (2026). Microstate dynamics of focused attention meditation. *Brain Topography*, 39(3), 40. https://doi.org/10.1007/s10548-026-01199-2

Price, M. M., Zanesco, A. P., Denkova, E., Barry, J., Rogers, S. L., & Jha, A. P. (2023). Investigating the protective effects of mindfulness-based attention training on mind wandering in applied settings. *Frontiers in Psychology*, *14*, 1232598. https://doi.org/10.3389/fpsyg.2023.1232598

Raichle, M. E. (2015). The brain's default mode network. *Annual Review of Neuroscience*, *38*(1), 433–447. https://doi.org/10.1146/annurev-neuro-071013-014030

Robertson, I. H., Manly, T., Andrade, J., Baddeley, B. T., & Yiend, J. (1997). 'Oops!': Performance correlates of everyday attentional failures in traumatic brain injured and normal subjects. *Neuropsychologia*, *35*(6), 747–758. https://doi.org/10.1016/S0028-3932(97)00015-8

Sadaghiani, S., & D'Esposito, M. (2015). Functional characterization of the cingulo-opercular network in the maintenance of tonic alertness. *Cerebral Cortex*, *25*(9), 2763–2773. https://doi.org/10.1093/cercor/bhu072

Schwartzman, B., Zanesco, A. P., Denkova, E., Tsukahara, J. S., & Jha, A. P. (2025). Examining the association between vigilance and mind wandering. *Frontiers in Cognition*, *4*, 1577053. https://doi.org/10.3389/fcogn.2025.1577053

Skrandies, W. (1990). Global field power and topographic similarity. *Brain Topography*, *3*(1). https://doi.org/10.1007/BF01128870

Society, A. E. (1991). American Electroencephalographic Society guidelines for standard electrode position nomenclature. *Journal of Clinical Neurophysiology*, *8*(2), 200–202. https://doi.org/10.1097/00004691-199104000-00007

Stanislaw, H., & Todorov, N. (1999). Calculation of signal detection theory measures. *Behavior Research Methods Instruments & Computers*, *31*(1), 137–149. https://doi.org/10.3758/BF03207704

Tarailis, P., Koenig, T., Michel, C. M., & Griskova-Bulanova, I. (2024). The functional aspects of resting EEG microstates: A systematic review. *Brain Topography*, *37*(2), 181–217. https://doi.org/10.1007/s10548-023-00958-9

Tarailis, P., Lory, K., Unschuld, P. G., Michel, C. M., & Brechet, L. (2025). Self-related thought alterations associated with intrinsic brain dysfunction in mild cognitive impairment.

Scientific Reports, *15*(1), 12279. https://doi.org/10.1038/s41598-025-97240-8

Thomson, D. R., Besner, D., & Smilek, D. (2015). A resource-control account of sustained attention: Evidence from mind-wandering and vigilance paradigms. *Perspectives on Psychological Science*, *10*(1), 82–96. https://doi.org/10.1177/1745691614556681

Unsworth, N. (2015). Consistency of attentional control as an important cognitive trait: A latent variable analysis. *Intelligence*, *49*, 110–128. https://doi.org/10.1016/j.intell.2015.01.005

Valt, C., Tavella, A., Berchio, C., Seebold, D., Sportelli, L., Rampino, A., Salisbury, D. F., Bertolino, A., & Pergola, G. (2024). Meg microstates: An investigation of underlying brain sources and potential neurophysiological processes. *Brain Topography*, *37*(6), 993–1009. https://doi.org/10.1007/s10548-024-01073-z

Warm, J. S., Parasuraman, R., & Matthews, G. (2008). Vigilance requires hard mental work and is stressful. *Human Factors*, *50*(3), 433–441. https://doi.org/10.1518/001872008X312152

Weissman, D. H., Roberts, K. C., Visscher, K. M., & Woldorff, M. G. (2006). The neural bases of momentary lapses in attention. *Nature Neuroscience*, *9*(7), 971–978. https://doi.org/10.1038/nn1727

Zainal, N. H., & Newman, M. G. (2024). Mindfulness enhances cognitive functioning: A meta-analysis of 111 randomized controlled trials. *Health Psychology Review*, *18*(2), 369–395. https://doi.org/10.1080/17437199.2023.2248222

Zanesco, A. P. (2024). Normative temporal dynamics of resting EEG microstates. *Brain Topography*, *37*(2), 243–264. https://doi.org/10.1007/s10548-023-01004-4

Zanesco, A. P., Denkova, E., Barry, J., & Jha, A. P. (2024). Mind wandering is associated with worsening attentional vigilance. *Journal of Experimental Psychology Human Perception and Performance*, *50*(11), 1049–1066. https://doi.org/10.1037/xhp0001233

Zanesco, A. P., Denkova, E., & Jha, A. P. (2021). Self-reported mind wandering and response time variability differentiate prestimulus electroencephalogram microstate dynamics during a sustained attention task. *Journal of Cognitive Neuroscience*, *33*(1), 28–45. https://doi.org/10.1162/jocn_a_01636

Zanesco, A. P., Denkova, E., & Jha, A. P. (2025). Mind-wandering increases in frequency over time during task performance: An individual-participant meta-analytic review. *Psychological Bulletin*, *151*(2), 217–239. https://doi.org/10.1037/bul0000424

Zanesco, A. P., Pandya, S., Denkova, E., & Jha, A. P. (2026). The dynamics of EEG microstates covary with spontaneous thoughts. *Cortex*, *197*, 34–56. https://doi.org/10.1016/j.cortex.2025.12.011

Zhang, H., Yang, S. Y., Qiao, Y., Ge, Q., Tang, Y. Y., Northoff, G., & Zang, Y. F. (2022). Default mode network mediates low-frequency fluctuations in brain activity and behavior during sustained attention. *Human Brain Mapping*, *43*(18), 5478–5489. https://doi.org/10.1002/hbm.26024